Radio Science, Volume 36, Number 1, Pages 1–8, January–February 2001

Characteristic-based time domain method for antenna analysis

Dan Jiao and Jian-Ming Jin

Center for Computational Electromagnetics, Department of Electrical and Computer Engineering
University of Illinois at Urbana-Champaign, Urbana, Illinois

J. S. Shang

Air Vehicles Directorate, Air Force Research Laboratory, Wright-Patterson Air Force Base, Ohio

Abstract. The characteristic-based time domain method, developed in the computational fluid dynamics community for solving the Euler equations, is applied to the antenna radiation problem. Based on the principle of the characteristic-based algorithm, a governing equation in the cylindrical coordinate system is formulated directly to facilitate the analysis of body-of-revolution antennas and also to achieve the exact Riemann problem. A finite difference scheme with second-order accuracy in both time and space is constructed from the eigenvalue and eigenvector analysis of the derived governing equation. Rigorous boundary conditions for all the field components are formulated to improve the accuracy of the characteristic-based finite difference scheme. Numerical results demonstrate the validity and accuracy of the proposed technique.

1. Introduction

A variety of numerical methods have been extensively investigated to model antenna radiation problems. Basically, they can be divided into two classes: time domain and frequency domain methods. Between them, the time domain method has received more attention recently than the frequency domain counterpart. There are several reasons for its popularity. First, the parameters of interest to characterize an antenna generally change drastically with frequency. When the traditional frequency domain methods are used for analysis, a set of algebraic equations must be solved repeatedly at many frequencies. This can be computationally expensive, and even become prohibitive, when an object of large electric size is considered. However, if the time domain method is employed, one simulation will be sufficient to generate all the information in the frequency domain. As a result, the time domain method greatly facilitates the modeling of antennas, especially the wideband antennas. Another attractive feature of the time domain method is that it solves the time-dependent Maxwell's equations directly and hence provides good physical insight into the radiation process. Furthermore, it removes the difficulty of handling material properties, which cannot be avoided easily by the frequency domain methods. Although the time domain method has to repeat the calculation for different incident angles when it deals with scattering problems, this is not the case in antenna radiation problems because here the excitation is often fixed, and the analysis usually requires one calculation.

In computational electromagnetics a popular time domain method is the finite-difference time domain (FDTD) method, which was developed by K. S. Yee in 1966 [*Yee*, 1966]. This method is a midpoint, leapfrog algorithm with second-order accuracy in both time and space domains. Since it is a central difference scheme, it does not induce any dissipation error, and hence it is neutrally stable [*Tannehill et al.*, 1997]. The inaccuracy induced by improper boundary conditions, the discretization error, and the round-off error will continuously propagate

Paper number 2000RS002339.
0048-6604/01/2000RS002339$11.00

through the entire computational domain. Since an absorbing boundary must be introduced to truncate the computation domain so that the infinite space can be simulated, the accuracy and stability of the FDTD scheme are restricted.

Maxwell's equations in time domain constitute a hyperbolic partial differential system, which is a pure initial value problem [*Sommerfeld*, 1949; *Courant and Hilbert*, 1965]. Therefore the characteristic-based algorithm [*Steger and Warming*, 1981; *Roe*, 1986], which was developed in the computational fluid dynamics community for solving the Euler equations, is found to be equally effective for solving Maxwell's equations in time domain [*Shang and Gaitonde*, 1995a, 1995b; *Shang*, 1995a, 1995b; *Shang and Robert*, 1996]. The basic approach of the characteristic-based method is to reduce the three-dimensional system of equations to an approximate Riemann problem in each spatial direction. The sequence of one-dimensional problems is then solved to obtain the solution to the original problem [*Shang*, 1995b]. The characteristic-based algorithm has several advantages over other time domain methods. First, it utilizes the unique feature of the hyperbolic differential system, which is that the given initial values, together with any possible discontinuities, are continued along the characteristics [*Sommerfeld*, 1949; *Courant and Hilbert*, 1965]. Consequently, if one of the coordinates of the system equation is aligned with the direction of the wave propagation, $\mathbf{E} \times \mathbf{H}$, the wave will continue to propagate along this direction, and hence no wave is reflected back. Therefore it naturally eliminates the reflected wave from the truncated outer boundary. Second, it enforces the directional propagation of information for wave motion, because it conducts a detailed eigenvalue analysis. Forward differencing is adopted for the negative eigenvalues, and the backward one is used for the positive eigenvalues. This windward discretization provides a more robust stability than a central differencing scheme, although second-order windward difference schemes are highly dissipative. Finally, the governing equation can be easily cast into a generalized curvilinear coordinate system. It greatly accommodates the computation of electromagnetic fields around a complex scatterer. The first and third features have been used by *Shankar et al.* [1989, 1990] in their finite volume time domain method for Maxwell's equations.

Because of the above advantages of the characteristic based algorithm it has been applied to solving electromagnetic problems in recent years [*Shang and Gaitonde*, 1995a, 1995b; *Shang*, 1995a, b; *Shang and Robert*, 1996]. From a survey of the literature it is found that the major concern at present is the scattering problem, and there has been little application of the method to antenna problems. However, it should be more advantageous to use this time domain method to deal with the radiation problem, because the position of the source is fixed and therefore it is not necessary to repeat the calculation for different incident angles. However, the application of the characteristic-based method to the antenna radiation problem is not straightforward if high accuracy is required. In this paper, a dipole antenna and a cylindrical monopole antenna are analyzed using the characteristic-based algorithm. In order to model these two kinds of antenna we first formulate a governing equation, which is feasible for the body-of-revolution (BOR) problem. With this governing equation the exact Riemann problem is then achieved, which enhances the accuracy of the numerical scheme. Next, a detailed eigenvalue and eigenvector analysis is conducted on the governing equation. A finite difference scheme with second-order accuracy in both time and space is constructed. Rigorous boundary conditions for all the field components on the surface of the perfect electric conductor (PEC) boundary are derived to improve the accuracy. Numerical examples are given to validate the proposed technique.

2. Formulation

If the characteristic-based algorithm is used directly for the analysis of a BOR antenna, the governing equation with six unknowns in Cartesian coordinates needs to be cast into the cylindrical coordinate system. This coordinate transformation induces errors in the characteristic-based scheme, since the exact Riemann problem cannot be achieved. It also introduces the artificial difficulty in the enforcement of the boundary condition on the surface of the antenna and on the outer boundary of the computational domain. In this paper, we start from Maxwell's equations in the cylindrical coordinate system directly. By choosing unknowns wisely, the exact Riemann problem can be achieved. At the same time, the difficulty in implementing the boundary conditions can be removed.

2.1. Governing Equations

For an antenna that is rotationally symmetric and excited by a rotationally symmetric source, the electromagnetic field is independent of the cylindrical coordinate ϕ. Therefore Maxwell's equations can be expressed as two independent sets: One involves only the components D_z, D_ρ, B_ϕ (transverse magnetic (TM) case), and the other involves only the components of B_z, B_ρ, and D_ϕ (transverse electric (TE) case). Taking the TM case as an example, the relevant Maxwell's equations become

$$\begin{aligned} \frac{\partial E_\rho}{\partial z} - \frac{\partial E_z}{\partial \rho} &= -\mu \frac{\partial H_\phi}{\partial t}, \\ -\frac{\partial H_\phi}{\partial z} &= \epsilon \frac{\partial E_\rho}{\partial t} + J_\rho, \\ \frac{1}{\rho}\frac{\partial (\rho H_\phi)}{\partial \rho} &= \epsilon \frac{\partial E_z}{\partial t} + J_z. \end{aligned} \tag{1}$$

Written in a flux vector form, the above equations become

$$\frac{\partial \mathbf{U}}{\partial t} + \frac{\partial \mathbf{F}_\rho}{\partial \rho} + \frac{\partial \mathbf{F}_z}{\partial z} = -\mathbf{J}, \tag{2}$$

$$\mathbf{U} = \begin{Bmatrix} \rho D_z \\ \rho D_\rho \\ \rho B_\phi \end{Bmatrix}, \tag{3}$$

$$\mathbf{F}_\rho = \begin{Bmatrix} -\rho B_\phi/\mu \\ 0 \\ -\rho D_z/\epsilon \end{Bmatrix}, \quad \mathbf{F}_z = \begin{Bmatrix} 0 \\ \rho B_\phi/\mu \\ \rho D_\rho/\epsilon \end{Bmatrix},$$

$$\mathbf{J} = \begin{Bmatrix} \rho J_z \\ \rho J_\rho \\ \rho D_z/(\rho\epsilon) \end{Bmatrix}. \tag{4}$$

Since the flux vectors $\mathbf{F}_\rho$ and $\mathbf{F}_z$ are homogeneous functions of degree 1 with respect to the dependent variable $\mathbf{U}$, they can be expressed as the product of the dependent variables and the coefficient matrices,

$$\mathbf{F}_\rho = A\mathbf{U}, \quad \mathbf{F}_z = B\mathbf{U}, \tag{5}$$

where the coefficient matrices A and B are

$$A = \begin{bmatrix} 0 & 0 & -\frac{1}{\mu} \\ 0 & 0 & 0 \\ -\frac{1}{\epsilon} & 0 & 0 \end{bmatrix}, \quad B = \begin{bmatrix} 0 & 0 & 0 \\ 0 & 0 & \frac{1}{\mu} \\ 0 & \frac{1}{\epsilon} & 0 \end{bmatrix}. \tag{6}$$

2.2. Eigenvalues and Eigenvectors

The characteristic-based algorithm conducts a detailed eigenvalue and eigenvector analysis. The equations in the flux vector form are correspondingly split according to the sign of the eigenvalues. The forward difference is applied to compute the flux vectors associated with the negative eigenvalue, and the backward difference is adopted to evaluate the flux vectors identified with the positive eigenvalue. This process mimics the wave mechanism of information propagation and hence provides a more robust stability than a central difference scheme.

The eigenvalues of the coefficient matrices A and B are the same, which are given by

$$\lambda = \left\{ 0, -\frac{1}{\sqrt{\mu\epsilon}}, \frac{1}{\sqrt{\mu\epsilon}} \right\}. \tag{7}$$

It is evident that the eigenvalues are nothing but the speed of the positively and negatively propagating waves.

The similarity matrices for diagonalization are constructed by using the eigenvectors as the column arrays as shown in the following equation:

$$S_A = \begin{bmatrix} 0 & \sqrt{\frac{\epsilon}{\mu}} & -\sqrt{\frac{\epsilon}{\mu}} \\ 1 & 0 & 0 \\ 0 & 1 & 1 \end{bmatrix},$$

$$S_B = \begin{bmatrix} 1 & 0 & 0 \\ 0 & -\sqrt{\frac{\epsilon}{\mu}} & \sqrt{\frac{\epsilon}{\mu}} \\ 0 & 1 & 1 \end{bmatrix}, \tag{8}$$

which leads to

$$\mathbf{F}_\rho = S_A \lambda S_A^{-1}\mathbf{U}, \quad \mathbf{F}_z = S_B \lambda S_B^{-1}\mathbf{U}. \tag{9}$$

From (7) and (8) it is obvious that the derived eigenvalues and eigenvectors are invariant with respect to the dependent variables $\mathbf{U}$. As a result, the exact Riemann problem can be achieved with this formulation.

2.3. Flux Vector Splitting

The fundamental idea of flux vector splitting is to process data according to the direction of wave propagation. The positively propagating wave is associated with the positive eigenvalue, and vice versa. As a consequence, the flux vectors $\mathbf{F}_\rho$ and $\mathbf{F}_z$ can be split as

$$\mathbf{F}_\rho = A^+\mathbf{U} + A^-\mathbf{U}, \tag{10}$$

$$\mathbf{F}_z = B^+\mathbf{U} + B^-\mathbf{U}, \tag{11}$$

$$A^+ = \begin{bmatrix} \frac{1}{2\sqrt{\epsilon\mu}} & 0 & -\frac{1}{2\mu} \\ 0 & 0 & 0 \\ -\frac{1}{2\epsilon} & 0 & \frac{1}{2\sqrt{\mu\epsilon}} \end{bmatrix},$$

$$A^- = \begin{bmatrix} -\frac{1}{2\sqrt{\epsilon\mu}} & 0 & -\frac{1}{2\mu} \\ 0 & 0 & 0 \\ -\frac{1}{2\epsilon} & 0 & -\frac{1}{2\sqrt{\mu\epsilon}} \end{bmatrix}, \quad (12)$$

$$B^+ = \begin{bmatrix} 0 & 0 & 0 \\ 0 & \frac{1}{2\sqrt{\epsilon\mu}} & \frac{1}{2\mu} \\ 0 & \frac{1}{2\epsilon} & \frac{1}{2\sqrt{\mu\epsilon}} \end{bmatrix},$$

$$B^- = \begin{bmatrix} 0 & 0 & 0 \\ 0 & -\frac{1}{2\sqrt{\epsilon\mu}} & \frac{1}{2\mu} \\ 0 & \frac{1}{2\epsilon} & -\frac{1}{2\sqrt{\mu\epsilon}} \end{bmatrix}. \quad (13)$$

A second-order accurate windward differencing can be constructed to form difference operators according to the sign of the eigenvalues,

$$\Delta \mathbf{U}_i = [-3\mathbf{U}_i + 4\mathbf{U}_{i+1} - \mathbf{U}_{i+2}]/2, \quad (14)$$

$$\nabla \mathbf{U}_i = [3\mathbf{U}_i - 4\mathbf{U}_{i-1} + \mathbf{U}_{i-2}]/2. \quad (15)$$

The fractional step method or the Runge-Kutta family of single-step multistage procedures can be employed to accomplish the time integration. In this paper, a single-step two-stage Runge-Kutta scheme is used to guarantee second-order accuracy in time.

2.4. Boundary Condition Implementation

For the analysis of the BOR antenna there are two kinds of boundary condition involved. One is the PEC boundary condition, and the other is the compatibility condition at the outer boundary of the computational domain.

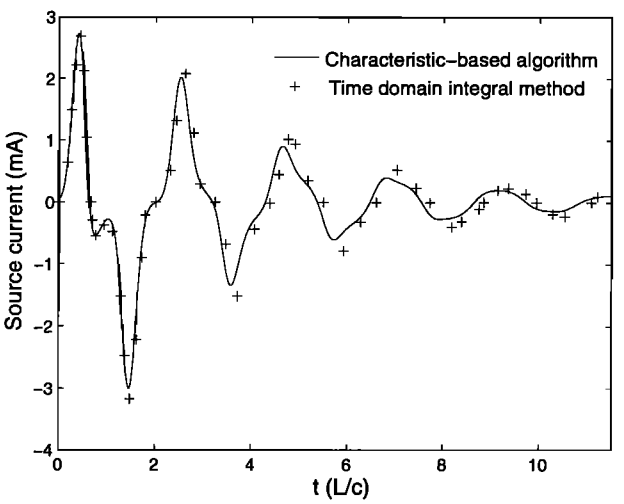

Figure 1. Electric current at the fed point of a center-fed dipole antenna with a Gaussian time-dependent voltage source.

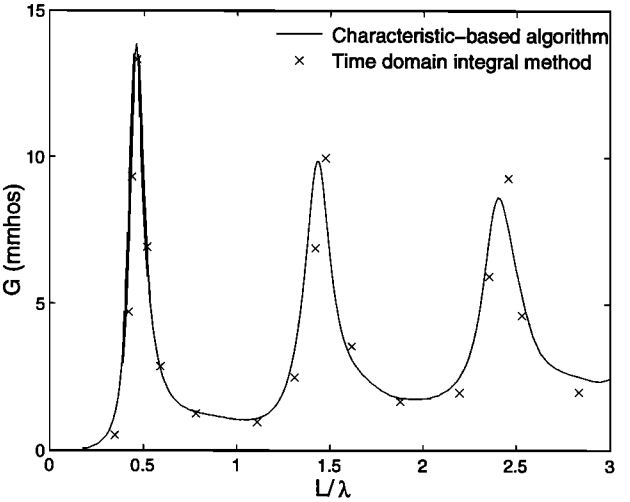

Figure 2. Conductance of a center-fed dipole antenna.

From Maxwell's equations it can be easily derived that on the side surface (parallel to the z axis) of the antenna body the following equations must be satisfied:

$$\frac{\partial(\rho H_\phi)}{\partial \rho} = 0, \quad E_z = 0, \quad \frac{\partial(\rho E_\rho)}{\partial \rho} = 0, \quad (16)$$

while at the end surfaces (perpendicular to the z axis) of the dipole or monopole antenna, the boundary conditions are

$$\frac{\partial H_\phi}{\partial z} = 0, \quad E_\rho = 0, \quad \frac{\partial E_z}{\partial z} = 0. \quad (17)$$

Since the governing equation is formed using ρD_ρ, ρD_z, and ρB_ϕ as unknowns, the above PEC boundary conditions can be easily cast into difference forms. The use of these unknowns also facilitates the enforcement of the field along the axis of the antenna.

At the outer boundary of the computational region an approximate no-reflection condition can be achieved by setting the incoming flux components to zero:

Right outer boundary $\mathbf{F}_\rho^- = 0$,
Upper outer boundary $\mathbf{F}_z^- = 0$,
Lower outer boundary $\mathbf{F}_z^+ = 0$.

To make the no-reflection condition effective, the truncated outer boundary should be placed several wavelengths away from the antenna. For cells whose stencil passes through the boundary the first-order windward stencil is utilized.

3. Numerical Examples

To demonstrate the validity of the proposed algorithm, a number of examples are considered here and the results are compared with other numerical or measured data. The first example is a linear, center-fed dipole antenna [*Poggio and Miller*, 1973]. The ratio of the radius to the length of the antenna, r/L, is equal to 0.00674. It is excited by a Gaussian time-dependent voltage source which takes the form of $V = \exp\,[-a^2(t - t_{\max})^2]$, where $a = 1.5 \times 10^9$ and $t_{\max} = 1.43 \times 10^{-9}$ s. The voltage source is fed to the antenna through a gap having a width of $L/20$ at the center of the antenna. On the basis of the equivalence principle the gap is filled with PEC, and a surface magnetic current M_ϕ is prescribed on the surface of the gap. This magnetic current is related to the voltage source by $M_\phi = V/d$, where d denotes the width of the gap; that is, $d = L/20$. The outer boundary of the computational domain is placed at a distance of L away from the antenna along both the ρ and z directions. The computational domain is discretized using two grid sizes. In the near region

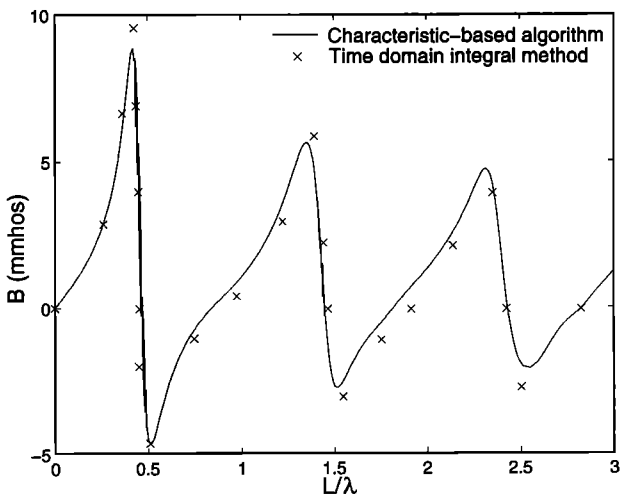

Figure 3. Susceptance of a center-fed dipole antenna.

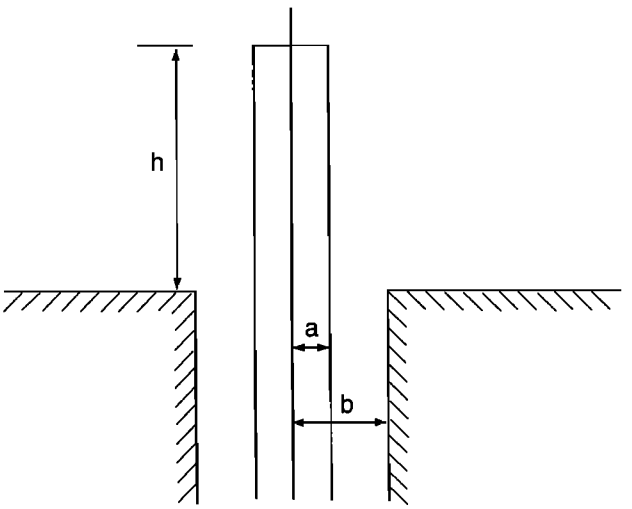

Figure 4. Geometry of a cylindrical monopole antenna fed through an image plane.

the discretization of 40 grids per wavelength is used, while in the far region the grid size is increased to be 20 grids per wavelength. Here, the wavelength corresponds to the maximum frequency of the incident pulse. To ensure stability, the time step is chosen to be $\Delta s/3c$, where Δs denotes the space step and c denotes the speed of light. The calculated current at the fed point is shown in Figure 1. By performing the Fourier transform on the source current and the excitation voltage the input admittance of the antenna can be obtained, which is shown in Figures 2 and 3. Clearly, the calculated result agrees well with the result from the time domain integral method [*Poggio and Miller*, 1973].

The second example considered here is a monopole antenna fed through an image plane from a coaxial transmission line [*Maloney et al.*, 1990], the geometry of which is shown in Figure 4. The parameters to characterize the monopole antenna are the height h and the radii of the inner and outer conductors of the coaxial line, a and b. In this example, the ratio of b to a is 2.3, and that of h to a is 32.8. The antenna is excited by the incident transverse electromagnetic (TEM) wave within the coaxial line, which is given by

$$E_\rho(t) = V^i(t)/\rho \ln\,(b/a), \qquad (18)$$
$$H_\phi(t) = V^i(t)/(2\pi\rho\eta),$$

where $\eta = 60 \ln\,(b/a)$ and

$$V^i(t) = \exp\,(-t^2/2\tau_p^2). \qquad (19)$$

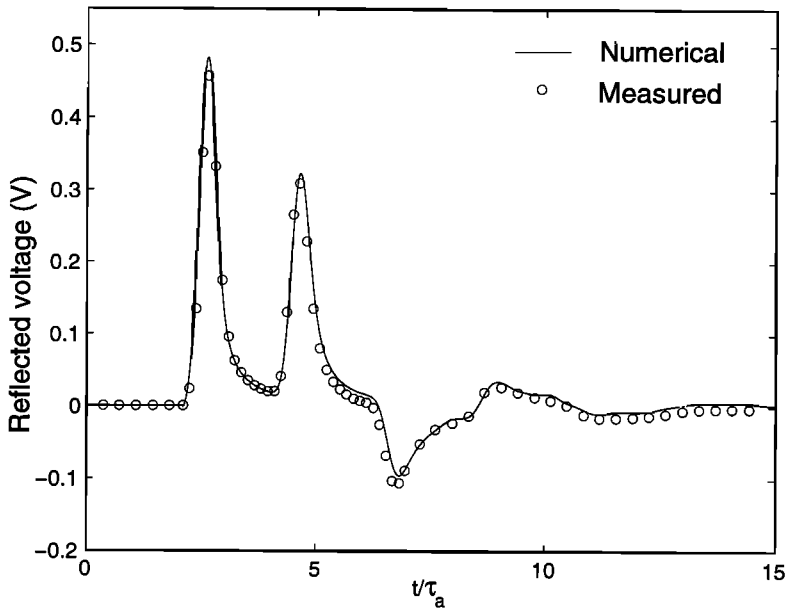

Figure 5. Reflected voltage in the coaxial line for a cylindrical monopole antenna excited by a 1 V Gaussian pulse: $b/a = 2.3$, $h/a = 32.8$, and τ_p/τ_a=0.161.

The internal reflection of the antenna is characterized by the time constant τ_a, which is equal to h/c. In order to compare with the measured data of *Maloney et al.* [1990] the ratio of τ_p to τ_a is chosen to be 0.161. To apply the compatibility condition, the outer boundary is placed at a distance of h away from the tip of the monopole and the outer edge of the coaxial line. The calculated reflected voltage in the coaxial line is shown in Figure 5. The reference plane to extract the reflected voltage can be chosen arbitrarily within the coaxial line, as long as only the TEM mode is present. The compatibility condition is also implemented here to suppress the incoming wave. From Figure 5 it can be seen clearly that the numerical result agrees very well with the measured data.

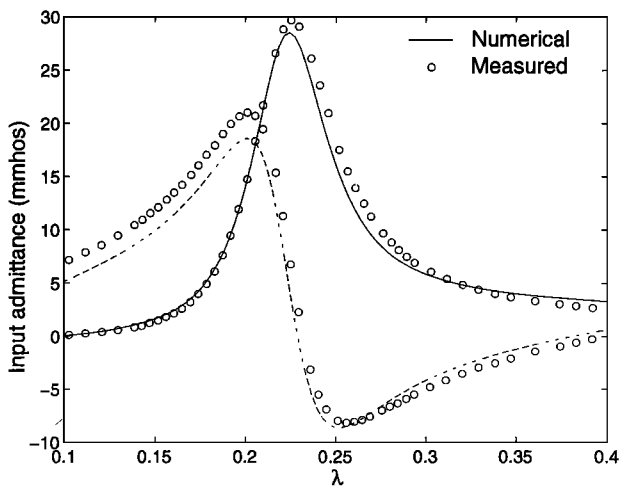

Figure 6. Input admittance of a cylindrical monopole antenna: $b/a = 3.0$.

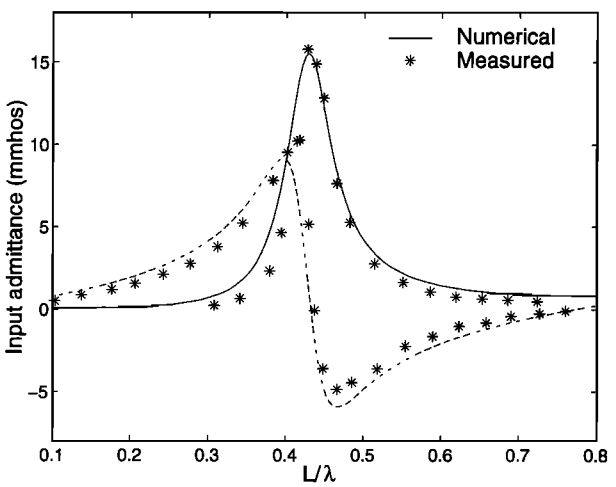

Figure 7. Input admittance of a dielectric coated dipole antenna: $L = 20.32$ cm, $2a = 0.063$ cm, $2b = 0.370$ cm, and $\epsilon_2 = 2.3\epsilon_0$.

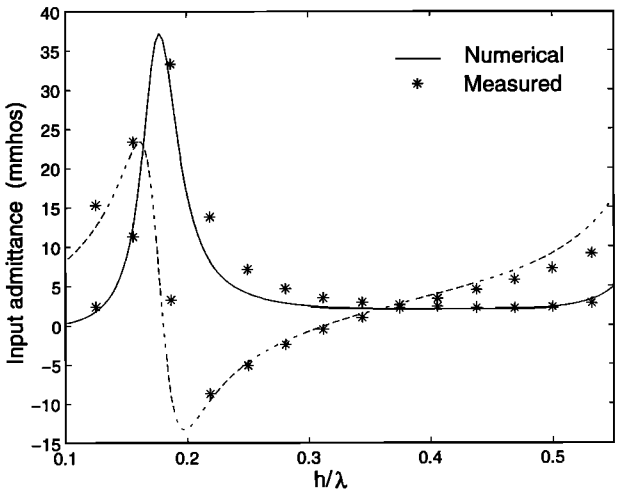

Figure 8. Input admittance of a dielectric coated monopole antenna: $2a = 0.63$ cm, $2b = 1.90$ cm, the diameter of the dielectric sleeve $d = 1.27$ cm, and $\epsilon_2 = 9.0\epsilon_0$.

Next, the input admittance of the monopole antenna is calculated. To compare with the result measured by *Cooper* [1975], the ratio of b to a is chosen to be 3.0. The Gaussian pulse in the form of (18) is still employed to excite the antenna. After extracting the reflected voltage within the coaxial line a Fourier transform is performed on it as well as on the incident voltage to obtain the reflection coefficient at the reference plane. From the reflection coefficient the input admittance at the aperture of the monopole antenna can be obtained. The result is shown in Figure 6, which exhibits a good agreement with the measured value.

The last two examples show the capability of the present method to deal with the electromagnetic interactions with materials. A special treatment as proposed by *Jiao et al.* [1999] is applied at the material interface to guarantee the tangential continuity of the electric and magnetic fields. A coated dipole antenna such as given by *Richmond and Newman* [1976] is first considered. The length of the antenna is 20.32 cm. The diameters of the antenna and the coating are 0.063 cm and 0.370 cm, respectively. The relative dielectric constant of the coating is 2.3. A Gaussian pulse with the same form as (18) is used to excite the antenna, and the calculated input admittance is shown in Figure 7. The next example is a coated monopole antenna [*Lamensdorf*, 1967]. The inner and outer diameters of the coaxial transmission line are 0.63 cm and 1.90 cm, respectively. The thickness of the dielectric sleeve is 0.32 cm with relative permittivity of 9.0. The dielectric sleeve is extended beyond the monopole to simulate an extension to infinity. Figure 8 shows the calculated input admittance, again compared with the measured data.

4. Conclusion

In this paper, a characteristic-based time domain scheme is presented for antenna analysis. In combination with the unique feature of the BOR antenna a governing equation is derived directly in the cylindrical coordinate system. It transforms the original initial and boundary value problem into an exact Riemann problem and hence improves the accuracy of the characteristic-based scheme in a non-Cartesian coordinate system. It also facilitates the enforcement of the PEC boundary conditions and compatibility condition. Numerical results are shown to demonstrate its effectiveness.

References

Cooper, L. J., Monopole antennas on electrically thick conducting cylinders, Ph.D. thesis, Harvard Univ., Canbridge, Mass., March 1975.

Courant, R., and D. Hilbert, *Methods of Mathematical Physics*, vol. 2, Wiley-Intersicence, New York, 1965.

Jiao, D., J. M. Jin, and J. S. Shang, Characteristic-based finite-volume time-domain method for scattering by coated objects, *Res. Rep.: CCEM-29-99*, Univ. of Illi., Oct. 21, 1999.

Lamensdorf, D. , An experimental investigation of dielectric coated antennas, *IEEE Trans. Antennas Propag.*, *15*, 767–771, 1967.

Maloney, J. G., G. S. Smith, and W. R. Scott, Accurate computation of the radiation from simple antennas using the finite-difference time-domain method, *IEEE Trans. Antennas Propag.*, *38*, 1059–1068, 1990.

Poggio, A. J., and E. K. Miller, Integral equation solutions of three dimensional scattering problems, in *Computer Techniques for Electromagnetics*, chap. 4, pp. 159-261, Permagon, Tarrytown, N. Y., 1973.

Richmond, J. H., and E. H. Newman, Dielectric coated wire antennas, *Radio Sci.*, *11*, 13–20, 1976.

Roe, P. L., Characteristic-based schemes for the Euler equations, *Annu. Rev. Fluid Mech.*, *18*, 337–365, 1986.

Shang, J. S., A fractional-step method for solving 3D, time-domain Maxwell equations, *J. Comput. Phys.*, *118*, 109–119, 1995a.

Shang, J. S., Characteristic-based algorithms for solving the Maxwell equations in the time domain, *IEEE Antennas Propag. Mag.*, *37*(3), 15–25, 1995b.

Shang, J. S., and D. Gaitonde, Characteristic-based, time-dependent Maxwell equations solvers on a general curvilinear frame, *AIAA J.*, *33*, 491–498, 1995a.

Shang, J. S., and D. Gaitonde, Scattered electromagnetic field of a reentry vehicle, *J. Spacecraft Rockets*, *32*, 294–301, 1995b.

Shang, J. S., and M. F. Robert, A comparative study of characteristic-based algorithms for the Maxwell equations, *J. Comput. Phys.*, *125*, 378–394, 1996.

Shankar V., W. Hall, and A. H. Mohammadian, A three-dimensional Maxwell's equation solver for computation of scattering from layered media, *IEEE Trans. Magn.*, *25*(4), 3098–3103, 1989.

Shankar, V., A. H. Mohammadian, and W. Hall, A time-domain, finite-volume treatment for the Maxwell equations, *Electromagnetics*, *10*(1-2), 127–145, 1990.

Sommerfeld, A., *Partial Differential Equations in Physics*, Academic, San Diego, Calif., 1949.

Steger, J. L., and R. F. Warming, Flux vector splitting of the inviscid gasdynamic equations with application to finite-difference methods, *J. Comput. Phys.*, *40*, 263–293, 1981.

Tannehill, J. C., D. A. Anderson, and R. H. Pletcher, *Computational Fluid Mechanics and Heat Transfer*, Taylor and Francis, Philadelphia, Pa., 1997.

Yee, K. S., Numerical solution of initial boundary value problems involving Maxwell's equations in isotropic media, *IEEE Trans. Antennas Propag.*, *14*, 302–307, 1966.

D. Jiao and J.-M. Jin, Center for Computational Electromagnetics, Department of Electrical and Computer Engineering, University of Illinois at Urbana-Champaign, 1406 W. Green Street, Urbana, IL 61801-2991. (e-mail: danjiao@uiuc.edu; j-jin1@uiuc.edu)

J. S. Shang, Air Vehicles Directorate, Air Force Research Laboratory, Wright-Patterson AFB, OH 45433-7913.

(Received February 11, 2000; revised July 3, 2000; accepted September 25, 2000.)